Physics Letters B 788 (2019) 192–197

Contents lists available at ScienceDirect

Physics Letters B

www.elsevier.com/locate/physletb

^{48}Si: An atypical nucleus?

Jia Jie Li [b], Wen Hui Long [a,*], Jérôme Margueron [c,d], Nguyen Van Giai [e]

[a] School of Nuclear Science and Technology, Lanzhou University, Lanzhou 730000, China
[b] Institut für Theoretische Physik, J. W. Goethe-Universität, D-60438 Frankfurt am Main, Germany
[c] Institute for Nuclear Theory, University of Washington, Seattle, WA 98195, USA
[d] Institut de Physique Nucléaire de Lyon, Université Claude Bernard Lyon 1, IN2P3-CNRS, F-69622 Villeurbanne Cedex, France
[e] Institut de Physique Nucléaire d'Orsay, Université Paris-Sud, Université Paris-Saclay, IN2P3-CNRS, F-91406 Orsay Cedex, France

ARTICLE INFO

Article history:
Received 24 July 2018
Received in revised form 20 November 2018
Accepted 20 November 2018
Available online 22 November 2018
Editor: J.-P. Blaizot

Keywords:
New magicity
Drip-line nucleus
Bubble-like structure
Pairing reentrance

ABSTRACT

Using the relativistic Hartree–Fock Lagrangian PKA1, we investigate the properties of the exotic nucleus ^{48}Si, which is predicted to be an atypical nucleus characterized by i) the onset of doubly magicity, ii) its location at the drip line, iii) the presence of dual semi-bubble structure (distinct central depletion in both of neutron and proton density profiles) in the ground state, and iv) the occurrence of pairing reentrance at finite temperature. While not being new for each, these phenomena are found to simultaneously occur in ^{48}Si. For instance, the dual semi-bubble structure reduces the spin–orbit splitting of low-ℓ orbitals and upraises the s orbitals, leading therefore to distinct $N = 34$ and $Z = 14$ magic shells in ^{48}Si. Consequently, the doubly magicities provide extra stability for such extreme neutron-rich system at the drip line. Associating with the neutron shell $N = 34$ and continuum above, the pairing correlations are reengaged interestingly at finite temperature. Theoretical nuclear modelings are known to be poorly predictive in general, and we asset our confidence in the prediction of our modeling on the fact that the predictions of PKA1 in various regions of the nuclear chart have systematically been found correct and more specifically in the region of pf shell. Whether our predictions are confirmed or not, ^{48}Si provides a concrete benchmark for the understanding of the nature of nuclear force.

© 2018 The Author(s). Published by Elsevier B.V. This is an open access article under the CC BY license (http://creativecommons.org/licenses/by/4.0/). Funded by SCOAP[3].

Closed-shell nuclei are particularly important for nuclear structure physics because the ground state of nuclei having proton or neutron numbers equal to magic numbers can be considered as an archetype of independent particles moving in a mean field potential. Theoretically, they provide crucial benchmarks for mean field properties using density functional approaches [1–3]. For instance, the spin–orbit (SO) coupling [4,5] and the approximate pseudospin symmetry (PSS) [6–8] play a crucial role in the occurrence of shell closure, and manifest the relativistic nature of the nuclear interaction [9,10]. The strong SO coupling existing in stable and near-stable nuclei is tightly related to the spatial gradient of nuclear potential which is originally determined by the density profile [1,2,11]. The alterations of the density profile from ordinary one, e.g., halo or central depletion, could modify the structure properties of exotic nuclei, such as the emergence of new magic shells as we will show in present study of ^{48}Si.

Over the past few decades significant progress in exotic nuclei has brought important changes in our view of finite nuclear systems. As one of the typical examples, magic numbers are not universal any more across the nuclear chart and they can change dramatically along with the degree of freedom of isospin, leading to novel and unexpected features [12–15]. A few of them include the collapse of the conventional magic numbers $N = 8$ and 20 in the islands of inversion [16–19]. New magic numbers can arise, as observed in the typical case of drip-line magic nucleus ^{24}O [20–22]. Recent observations on new magic shells in proton- and neutron-rich nuclei are summarized in Fig. 1. These experimental achievements have demonstrated the idea that shell evolution in nuclei comes from a combination of complex effects related to the nuclear force.

More specifically in neutron-rich pf-shell nuclei, intensive efforts have been devoted to the occurrence of new magic shells at $N = 32$ and 34. The magicity at $N = 32$ have been signed from the measurements of the 2_1^+ excitation energy in titanium, chromium and calcium isotopes [23–25], and further confirmed by the high-precision mass measurements of exotic calcium and

* Corresponding author.
E-mail address: longwh@lzu.edu.cn (W.H. Long).

https://doi.org/10.1016/j.physletb.2018.11.034
0370-2693/© 2018 The Author(s). Published by Elsevier B.V. This is an open access article under the CC BY license (http://creativecommons.org/licenses/by/4.0/). Funded by SCOAP[3].

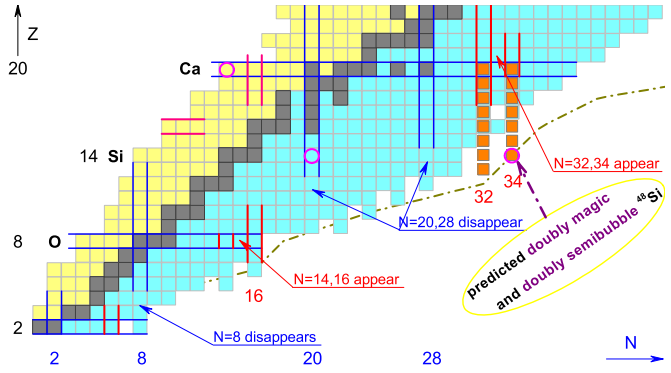

Fig. 1. Recent observations of the evolution of magicity, updated from Ref. [14]. Some isotopes of interest here are indicated in black. The green dashed-dotted line shows the average drip line predicted by relativistic energy density functionals [40]. The orange squares stand for the $N = 32$ and 34 isotones with $Z \leq 20$. The three pink circles mark the expected bubble-like nuclei ^{34}Ca and ^{34,48}Si [41–43].

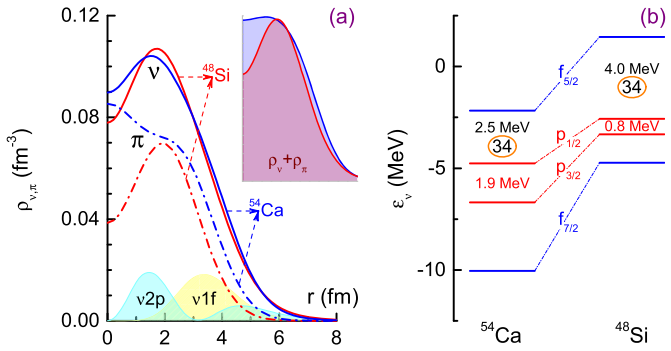

Fig. 2. Baryonic density distributions (a) and neutron single-particle spectra (b) for the ground states of ^{48}Si and ^{54}Ca, calculated by RHFB with PKA1. The compositions of $\nu 2p$ and $\nu 1f$ for ^{48}Si are also shown. The shell gaps of interest are indicated.

potassium isotopes [26,27]. The magicity at $N = 34$ was revealed from the measurement of the 2_1^+ energy in ^{54}Ca [28,29], and theoretically supported by ab-initio calculations [30,31], shell models [29,32], and some density functionals containing tensor terms [33–35]. Very recently, the mass evolution in calcium isotopes beyond $N = 34$ indicated again the magicity at $N = 34$ [36]. Since the new magic numbers $N = 32$ and 34 in calcium isotopes are now well established, it's natural to examine how they evolve in more exotic regions, e.g., in the $N = 32$ and 34 isotones with less protons. Shell model calculations have predicted a larger $N = 34$ shell gap in ^{52}Ar than the one reported in ^{54}Ca [32], and an increasing of the 2_1^+ energies in argon, sulfur and silicon isotopes from $N = 32$ to 34 [37]. It has also been shown from the relativistic approach that the $N = 34$ shell gaps are continuously enhanced from ^{52}Ar to ^{48}Si, indicating ^{48}Si as a new drip-line magic nucleus [35]. Notice further that this nucleus is expected to be spherical or weakly deformed by most of the modern nuclear density functionals [38–40].

The last identified silicon isotope to date is ^{44}Si [44], with four neutrons less than ^{48}Si. The synthesis of ^{48}Si is however a major challenge which may not be overcome in the near future. A possibility scenario for the production of more exotic silicon isotopes may be based on the new heavy-ion-induced nucleon-exchange reactions [45], which could lead to secondary nuclei with more neutrons than the primary beam. While we have assessed the difficulties in the synthesis of ^{48}Si, the purpose of present study is to illustrate, from a theoretical viewpoint, that ^{48}Si can be a very important nucleus to benchmark the present nuclear models and interactions. To our knowledge, the interest in the exploration of silicon isotopes is based on three observations: i) the existence of the new shell closure $Z = 14$ in ^{34}Si [46,47], ii) the disappearance of the $N = 28$ shell closure in ^{42}Si [48,49], and iii) the onset of a proton semi-bubble structure (reduced density at the nuclear interior) in ^{34}Si [41–43,50]. For the formation of semi-bubble it is in general required that the nucleus be spherical or just weakly deformed, and sometimes also has weak pairing correlations, to ensure a low population of s orbital. In principle, a central depletion in density profile can reduce the depth of potential well and present substantial contribution to the SO potential in the central region, while opposite to the trend at surface area [11,41]. In this work we present the illustrative prediction that such a central depletion in density profile may associate essentially with the characteristic of the single-particle (s.p.) structure, i.e., the occurrence of a new magicity.

In connection to our analysis, it is interesting to mention a recent correlation analysis [51] which shows that the central density in medium-mass nuclei carries little information on the properties of nuclear matter since it is predominantly driven by shell structure. We can therefore deduce that for the silicon isotopes, the dominant properties are impacted more by the finite size effects such as surface properties, and the specific details including finite range feature of the nuclear interaction, rather than the global ones reflected by the mean field approximation of nuclear matter. In our present analysis, this remark provides an additional argument for the promotion of nuclei such as ^{48}Si to benchmark nuclear modeling.

Let us start with the discussion of the $N = 34$ and $Z = 14$ new magicities as predicted from the relativistic Hartree–Fock–Bogoliubov (RHFB) approach considering spherical symmetry [35,52]. The coupled integro-differential RHFB equations are solved on the Dirac Woods–Saxon basis [53] with a radial cutoff $R = 28$ fm. In the pairing channel, the Gogny force D1S [54] is slightly adjusted — by a few percent correction — with a global strength factor, so as to reproduce the odd–even mass differences of calcium isotopes and $N = 28$ isotones. This model is well suited for the description of the density profile from the center to the most external part of nuclei. We base our predictions on the PKA1 Lagrangian [55] including the exchange of π (pseudovector), ω (vector), σ (scalar) and ρ (vector, tensor) mesons, as well as the density-dependent meson–nucleon couplings. The nuclear tensor force is naturally taken into account by the Fock diagrams [35,55,56]. The $N = 34$ shell gaps are predicted to be ~ 2.5 and 4.0 MeV, respectively, for ^{54}Ca and ^{48}Si [35], being consistent with the shell model calculations [32,37]. In addition, it is found that the tensor ρ and pseudovector π meson–nucleon couplings, which can be treated as a mixture of central and tensor forces, are the important ingredients in relativistic density functional to reproduce the evolutions of the s.p. spectrum for both sd- and pf-shell nuclei [35,41]. These results exemplify that the PKA1 Lagrangian furnishes a optimal choice for discussing the properties of very neutron-rich nuclei, such as ^{48}Si.

The neutron (ν) and proton (π) density profiles for the $N = 34$ isotones ^{54}Ca and ^{48}Si are shown in Fig. 2(a). We observe a central depletion in both neutron densities of ^{54}Ca and ^{48}Si. In ^{54}Ca, the valence neutrons, i.e., the $\nu 2p_{3/2,1/2}$ and $\nu f_{7/2}$ orbitals, dominate the formation of a weak neutron central depletion by raising the density profile beyond the center. Such density profile is not sensitive to the pairing correlations since the next neutron s orbital (i.e., $\nu 3s_{1/2}$) is far above the Fermi level. In ^{48}Si, additional effects from the proton sector enhance the neutron central depletion; we shall further discuss it later (regard to Fig. 3). There is however an important difference between the proton densities of ^{54}Ca and ^{48}Si, leading to qualitatively very different total density distributions. In

^{54}Ca the proton density exhibits a small central bump, which compensates the central depletion of neutron to give central flat total density. On the contrary, evident bubble-like structure appears in proton density profile of ^{48}Si, which in turn makes ^{48}Si as one of the rare but possible candidates — dual semi-bubble nucleus — with both neutron and proton bubble-like structures. In addition, a comparably large (~ 5.0 MeV) proton gap $Z = 14$ is found as in the doubly magic nucleus ^{34}Si [41,43]. In fact, as described by ordinary mean field models [1], ^{48}Si has similar proton configuration as ^{34}Si [41,43,47]: the last occupied proton orbital is $\pi 1d_{5/2}$, above which the $\pi 2s_{1/2}$ is essentially empty. Such configurations usually occur in nuclei with a central-depressed density profile because of the lack of an s state contribution [11,41,50,57]. It is therefore a quantum shell effect, at variance with bubble-like structure in superheavy nuclei powered by the Coulomb interaction [41,58–60]. This quantum effect can however be weakened by correlations beyond the mean field. If for instance the s-state is close enough to the last occupied state, pairing [41,50,57,61] as well as multi-reference framework beyond mean field [62,63] may populate the s-state with a non-zero probability, washing out the central depletion. The size of the energy gap between the last occupied state and the next s-state is therefore a crucial quantity to assess the prediction of a bubble-like structure.

In ^{48}Si, the existence of large proton gap (~ 5.0 MeV) is a rather clear argument in favor of the occurrence of proton semi-bubble structure, in addition to ^{34}Si [41,43]. Similar prediction is also made by the Skyrme-HFB calculation from the BRUSLIB database [64]. Notice however that while protons are predicted to have a central depletion in ^{48}Si from the BRUSLIB database, the neutrons are not. This indicates the model dependence of such prediction and emphasizes its importance to better understand the nature of nuclear forces. The isoscalar sector of the nuclear density functional is well constrained by available nuclear observables, but the isovector sector remains poorly determined. The difference between our predictions and the BRUSLIB (Skyrme interaction) ones might however be traced back to the difference in the isovector sector of interactions. For instance, the symmetry energy and its slope at saturation density from Skyrme density functionals are in general smaller than those from relativistic density functionals.

Let us recall that, in mean field approaches the SO interaction scales with the derivative of nuclear potential, and consistently with that of nucleon densities [1–3]. For relativistic mean field approaches, the derivative of the isoscalar (total) density dominates the SO effects, while that of the isovector density (difference between neutron and proton densities) contributes additional but much smaller corrections [65]. Specifically, the positive radial gradient, represented by the central depletion of nucleon density, partly compensates the negative one at the surface of nucleus, leading to a reduced SO splitting for low-ℓ orbitals [11, 41,50,57]. As observed in Fig. 2(b), the $\nu 2p$ splitting is reduced from ~ 1.9 MeV in ^{54}Ca (central depletion in the neutron density but not in the total one) down to ~ 0.8 MeV in ^{48}Si (dual semi-bubble candidate). One may notice that the reduction of $\nu 2p$ splitting ($\sim$1.1 MeV) cannot entirely account for the enlargement of the $N = 34$ shell gap (increase by $\sim$1.5 MeV from ^{54}Ca to ^{48}Si), since the $\nu 1f$ splitting is slightly reduced as well, see Fig. 2(b). Another effect contributing to the opening of the $N = 34$ shell gap is related to the enlarged splitting of the pseudospin (PS) partners $\{\nu 1f_{5/2}, \nu 2p_{3/2}\}$ from ^{54}Ca to ^{48}Si, which can be interpreted also by the semi-bubble structure that in general leads to evident violation of the PSS [2,9,10,66,67]. In conclusion, a dual semi-bubble structure predicted in ^{48}Si is illustrated to occur simultaneously with the distinctly reduced SO splitting of $\nu 2p$ and the enlarged PS splitting of $\{\nu 1f_{5/2}, \nu 2p_{3/2}\}$, coherently triggering the emergence of a fairly large $N = 34$ shell gap of ~ 4 MeV. Furthermore,

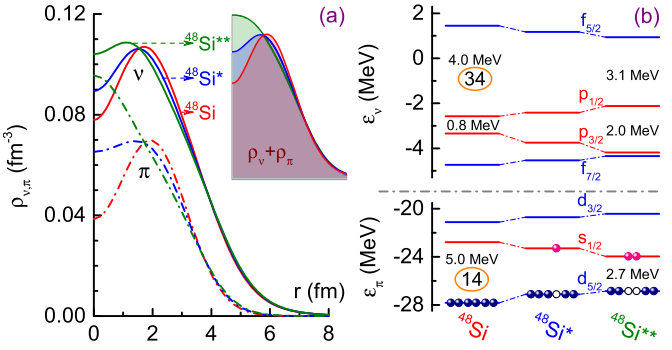

Fig. 3. Baryonic density distributions (a) and single-particle spectra (b) in the ground and excited configurations for ^{48}Si, calculated by RHFB with PKA1. Notice that the ordering of the density distributions according to their configurations depends on the radial interval. The shell gaps of interest are indicated. See the text for details.

the central depletion in the total density of ^{48}Si, corresponding to a central-bumped nuclear potential, tends to upraise the proton $\pi 2s_{1/2}$ orbital, and thus promotes the formation of a distinct proton $Z = 14$ shell (the energy gap between $\pi 1d_{5/2}$ and $\pi 2s_{1/2}$).

The influence of the dual semi-bubble on the $N = 34$ and $Z = 14$ shell gaps is further analyzed in Fig. 3 where we compare the predicted ground state of ^{48}Si with the excited ones ^{48}Si* and ^{48}Si**, in which $\pi 2s_{1/2}$ is partially and fully occupied, respectively. As expected, the proton central density becomes flat in ^{48}Si* and the neutron one still manifests a depletion, reducing partly the bubble-like structure in ^{48}Si* compared to ^{48}Si. Whereas in ^{48}Si** the proton central density manifests a distinct bump and the neutron one is flat, washing out completely the central depletion in the total density, see Fig. 3(a). Combining Figs. 3(a) and (b) it is evident that there exists indeed a clear relation between the sizes of $N = 34$ and $Z = 14$ shell gaps and the central density profile: semi-bubble structure favors the magicities when the low-ℓ orbitals like s and p are involved in determining the shells. One may also notice that the $\nu 2p$ splitting in ^{48}Si** is as large as that in ^{54}Ca, see Fig. 3(b). This is certainly due to the fact that the total density of ^{48}Si** is close to flat. Furthermore, the effects of neutron–proton interaction tend to make the proton and neutron density profile rather similar, as illustrated in Fig. 3(a). At variance with ^{54}Ca for which the valence neutrons dominate the formation of the semi-bubble, the neutron–proton interaction plays a key role in ^{48}Si.

There is another interesting effect in ^{48}Si* (or ^{48}Si**) for the SO splitting of larger-ℓ states. The increasing of the neutron (proton) central density induces a small modification of its asymptotic behavior, as observed in Fig. 3(a): the gradient of the peripheral nucleon density is smaller in ^{48}Si* (or ^{48}Si**) compared to ^{48}Si. Since the $\nu 1f$ states have a larger overlap with the nuclear surface than with the interior region, contrarily to the $\nu 2p$ states, the SO splittings of these larger-ℓ states get smaller going from ^{48}Si towards ^{48}Si* (or ^{48}Si**). Consequently the PS splitting for partners $\{\nu 1f_{5/2}, \nu 2p_{3/2}\}$ is somewhat enlarged. Therefore, the $N = 34$ gap in ^{48}Si** (~ 3.1 MeV) is still larger than that in ^{54}Ca (~ 2.5 MeV). The trends discussed on neutron sector can also be seen in proton sector. With the increasing of central density, consistently deepening of potential well, the SO splitting of $\pi 1d$ is slightly reduced, meanwhile the PS splitting of $\{\pi 1d_{3/2}, \pi 2s_{1/2}\}$ is remarkably enlarged because s orbital becomes more bound. As a result, the $Z = 14$ shell is quenched in ^{48}Si**, see Fig. 3(b).

To summarize, the comparison of our predictions for the ground state of ^{48}Si and the excited states ^{48}Si* and ^{48}Si** clearly illustrates the close relation between i) the central depletion in the density profile and the reduction of SO splitting of low-ℓ orbitals,

as well as the increase of the splitting of PS doublet nearby, and ii) the reduction of the external density profile and the decrease of the SO splitting of the larger-ℓ orbitals. The mechanism for the SO reduction is the same as the one described for other semi-bubble nuclei [11,41] and observed in ^{34}Si [43]. Notice however that in Refs. [11,41] the variation of SO splitting are mainly assessed by comparing the difference between two neighboring nuclei with s orbital populated or not. The PSS plays also an important role in conjunction with the onsets of both dual semi-bubble structure and new magic shells $N = 34$ and $Z = 14$. ^{48}Si is therefore a special nucleus, in which the onset of the dual semi-bubble structure induces various SO and PS couplings which coherently add together to strengthen the new magic shells. As a supplementation, the calculations with Hartree–Fock Lagrangians PKO1,3 [68,69], and with Hartree ones DD-ME2 [70] and PK1 [71] were also preformed. The dual semi-bubble structure in ^{48}Si is found to be rather common and, the enhancement of $N = 34$ shell gap from ^{54}Ca to ^{48}Si is also confirmed. While it should be mentioned that the $N = 34$ shell gap in ^{48}Si predicted by these Lagrangians is less pronounced than that given by PKA1, and coincidentally they already failed to reproduce the magicity in ^{54}Ca.

Let us open a parenthesis on superheavy and hyperheavy nuclei, in which similar coupling between the onset of a bubble-like (or bubble) structure and the opening of new magic shell may play certain role. These nuclei lie beyond the currently known region of the nuclear chart and may also take the form of (semi-)bubbles [41,58–60]. In superheavy nuclei with $Z \sim 120$, the polarization due to high-ℓ orbitals and large Coulomb repulsion generate a central-depressed matter distribution. This makes large shell gaps possible at $Z = 120$, which corresponds to the large PS splitting of doublet $\{\pi 2f_{5/2}, \pi 3p_{3/2}\}$ coincident with the collapse of the $\pi 3p$ splitting [41,58,72]. Although the mechanism producing the semi-bubble shape in ^{48}Si and $Z = 120$ superheavy nuclei is different, it is interesting to stress that the magicity in these two systems may originate from the same root: the occurrence of a bubble-like structure due to the quantum orbital effects, via reducing the SO splitting and enhancing the splitting between PS partners simultaneously, may trigger the opening of strong shell gap.

In the last part of this Letter, we now focus on the thermal excitation of ^{48}Si. It is well recognized that the coupling to the continuum, particularly the low-lying s.p. resonant states, becomes more and more important as nuclei get close to the drip lines [2,73,74]. For drip-line nuclei the structure of the s.p. continuum, apart from its interplay with magicity, can affect the location of the drip line itself [73–75]. In ^{48}Si we also find the continuum has an interesting structure that a few resonant states are located just above the $N = 34$ shell. This structure allows a novel phenomenon to occur in ^{48}Si, the pairing reentrance at finite temperature. In addition to the recently revealed ones ^{48}Ni [76] and ^{176}Sn [77], ^{48}Si can be the third candidate for such phenomenon. To show this, we employ the finite-temperature RHFB approach developed in Ref. [78].

At zero and very low temperatures ^{48}Si is expected to be and to remain unpaired because of the distinct magicity. At finite temperature, however, thermal excitations may populate the orbitals above Fermi level with certain probability. For ^{48}Si, the relevant states are the valence neutron orbitals $\nu 2p_{1/2,3/2}$ and $\nu 1f_{7/2}$, and the continuum states above the shell $N = 34$. The spreading of valence neutrons over these orbitals at finite temperature may switch on pairing correlations, leading to the so-called pairing reentrance. Since this phenomenon is going against the general expectation that the effect of thermal dynamics destroys pairing, it may take place only below the usual critical temperature in finite nuclei, ~ 1.0 MeV [77–79]. In Fig. 4(a), we represent the neutron and proton pairing gaps $\Delta_{\nu,\pi}$ for ^{48}Si as a function of temperature. Two critical temperatures, corresponding to the low- and high-temperature boundaries of pairing reentrance, are predicted to be $T_{c1} \sim 0.15$ MeV and $T_{c2} \sim 0.9$ MeV. Outside this range, neutrons are in the normal (unpaired) phase. It is worth noticing that protons also manifest pairing reentrance which appears from $T \sim 0.2$ MeV and quenches at $T \sim 0.5$ MeV, but the effects are negligible. This is because i) the proton $Z = 14$ shell is more robust than the neutron $N = 34$ one and ii) the relevant valence proton states around the Fermi level are much less than those of neutron's because of the presence of $Z = 20$ shell above.

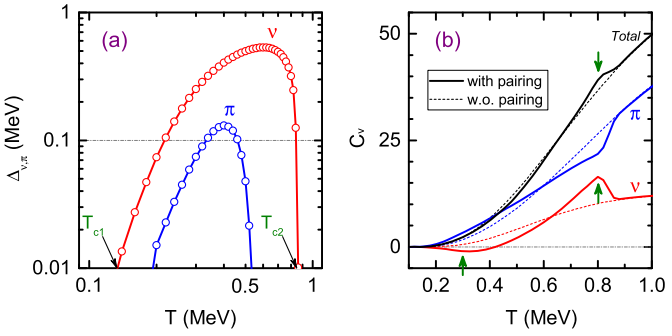

Fig. 4. Pairing gap (a) and specific heat (b) for ^{48}Si as a function of temperature T, calculated by finite-temperature RHFB with Lagrangian PKA1 and Gogny pairing force D1S [54]. The signatures for phase transition are marked by arrows. See the text for details.

The specific heat C_V reflects the second derivative of the free energy with respect to the temperature and it is thus sensitive to the thermal excitations of nucleus. Fig. 4(b) shows the specific heats obtained by switching on and off the pairing correlations for ^{48}Si. In the case where pairing is artificially switched off (in dashed lines), the specific heats of normal phase are almost a linear function of temperature. In the case where the pairing is determined self-consistently (in solid lines), the specific heats of superfluid phase present considerable difference with respect to those of normal phase, especially, the neutron specific heat demonstrates a non-monotonous variation with temperature. As the pairing correlations rebuilt after T_{c1}, the neutron specific heat is suppressed with respect to the normal phase (see the lowest arrow), and afterwards it is distinctly enhanced with respect to normal phase, showing a clear bump around $T = 0.8$ MeV (see the second arrow). This peculiar behavior of the specific heat between T_{c1} and T_{c2} can be considered as a signature of pairing reentrance. Moreover, although protons present rather weak pairing, their specific heat is also different from the normal phase, showing that protons are sensitive to the phase transition occurring in the neutron channel since they are cross-interacting. Notice that the proton and neutron specific heats vary with opposite behaviors between T_{c1} and T_{c2}, thus reducing the impact of the neutron superfluidity in the total specific heat. There is, therefore, a weak but still visible bump in the total specific heat at $T \sim 0.8$ MeV (see the third arrow).

In our framework, particle number is imposed only on average from the chemical potential. It has been shown within the Bardeen–Cooper–Schrieffer (BCS) approximation including particle number restoration that, in some cases, doubly magic nuclei could be weakly paired even in their ground state [80,81]. This is an interesting additional effect which is not included in our framework, but this prediction does not go against our prediction at finite temperature, since these two kinds of correlations — particle number restoration and finite temperature — both act towards the same direction: enhancement of pairing correlations. In the future, it will however be interesting to perform a finite-temperature RHFB calculation with particle number restoration.

The confirmation of pairing reentrance in ^{48}Si represents very challenging predictions for both nuclear physics rare-isotope beam facilities and theoretical developments at the frontier of stability. Signatures of pairing reentrance may be low-temperature anomalies of the specific heat or of the level density, or even might be deduced from pair transfer reaction mechanism [82,83]. Interestingly, a similar phenomenon called pairing persistence [77,78] was recently predicted from finite temperature approaches and may occur in less exotic nuclei, close to subshell closure. The pairing persistence leads to an increase of the critical temperature beyond the usual BCS limit, powered by thermally excited states around the Fermi level. At low temperature (below ~ 1.0 MeV) pairing can persist beyond the BCS limit due to the structure of the excited states. The mechanism for pairing persistence and pairing reentrance is therefore similar in nature, while occurring in different systems.

In summary, by employing the RHFB Lagrangian PKA1, we predict that ^{48}Si may be the next *doubly magic drip-line* nucleus. Our prediction is however partly model dependent and other Lagrangians such as the PKOi series produce less evident magicity at $N = 34$. Note that the PKOi series are less complete in the kind of interacting vertex than the PKA1 Lagrangian and have already proven difficulties in reproducing recent observables in neutron-rich nuclei that PKA1 could reproduce [35,41]. Independently of the model themselves, one can remark that ^{48}Si is at the intersection between new magicities observed for neutrons and protons, i.e., $Z = 14$ in neutron-rich light nuclei [42,43] and $N = 34$ expected from measurements in ^{54}Ca [29,36]. ^{48}Si is also predicted to be the first candidate of *dual semi-bubble* nucleus with both neutron and proton bubble-like shapes. A novel mechanism for the opening of new magicities is illustrated in this Letter, where the dual bubble-like structure produces a reduction of the SO splitting and an increase of the PS splitting, which coherently lead to the $N = 34$, $Z = 14$ shell gaps in ^{48}Si. We suggest that measurements of $E(2_1^+)$ and $B(E2)$ values in isotones close to ^{48}Si, such as ^{50}S for instance, will already provide trends which could be compared to theoretical predictions. It is appealing to notice that new neutron-rich nuclei, such as ^{47}P, ^{49}S, close to the drip lines have been discovered very recently [84].

Moreover, ^{48}Si is potentially one of the very few nuclei for which *pairing reentrance* occurs at finite temperature. The occurrence of such phenomenon depends sensitively on the structure of the s.p. spectrum, like the size of the shell gap and the type of resonant states, which impacts the values for the critical temperatures T_{c1} and T_{c2}, as well as the temperature dependence of the specific heat. There is therefore a strong model dependence in our prediction, for instance, the PKOi series predict pairing persistence instead of reentrance at finite temperature. The weakly bound ^{48}Si nucleus is only four neutrons beyond the heaviest isotope presently observed, ^{44}Si, making it yet unknown but probably accessible for the next generation of radioactive ion beam facilities. We have shown that ^{48}Si may be a very atypical nucleus benchmarking theoretical modeling. The confirmation or the refutation of our predictions for the ground state and excited states of ^{48}Si represents therefore both an experimental and theoretical challenge for the understanding of the nature of nuclear forces.

Finally, we should mention that the deformation, that leads to different s.p. structure from spherical case, may quench the bubble-like profile. To further examine the properties of ^{48}Si, it is important to perform the RHFB calculations by imposing (at least) axial symmetry. While due to the complexity induced by Fock terms, particularly for the ρ-tensor coupling in PKA1, such calculations are not as trivial as the RHB case. This perspective is in progress and will be reported in the future.

Acknowledgements

This work is partly supported by the National Natural Science Foundation of China under Grant No. 11675065. J.L. acknowledges the support by the Alexander von Humboldt Foundation.

References

[1] M. Bender, P.-H. Heenen, P.-G. Reinhard, Rev. Mod. Phys. 75 (2003) 121–180.
[2] J. Meng, H. Toki, S.G. Zhou, S.Q. Zhang, W.H. Long, et al., Prog. Part. Nucl. Phys. 57 (2006) 470–563.
[3] H. Sagawa, G. Colò, Prog. Part. Nucl. Phys. 76 (2014) 76–115.
[4] M.G. Mayer, Phys. Rev. 74 (1948) 235–239.
[5] O. Haxel, J.H.D. Jensen, H.E. Suess, Phys. Rev. 75 (1949) 1766.
[6] A. Arima, M. Harvey, K. Shimizu, Phys. Lett. B 30 (1969) 517–522.
[7] K.T. Hecht, A. Adler, Nucl. Phys. A 137 (1969) 129–143.
[8] J.N. Ginocchio, Phys. Rev. Lett. 78 (1997) 436–439.
[9] J.N. Ginocchio, Phys. Rep. 414 (2005) 165–261.
[10] H. Liang, J. Meng, S.-G. Zhou, Phys. Rep. 570 (2015) 1–84.
[11] B.G. Todd-Rutel, J. Piekarewicz, P.D. Cottle, Phys. Rev. C 69 (2004) 021301.
[12] A. Gade, T. Glasmacher, Prog. Part. Nucl. Phys. 60 (2008) 161–224.
[13] O. Sorlin, M.-G. Porquet, Prog. Part. Nucl. Phys. 61 (2008) 602–673.
[14] I. Tanihata, H. Savajols, R. Kanungo, Prog. Part. Nucl. Phys. 68 (2013) 215–313.
[15] T. Otsuka, Phys. Scr. T 152 (2013) 014007.
[16] I. Tanihata, H. Hamagaki, O. Hashimoto, Y. Shida, N. Yoshikawa, et al., Phys. Rev. Lett. 55 (1985) 2676–2679.
[17] E.K. Warburton, J.A. Becker, B.A. Brown, Phys. Rev. C 41 (1990) 1147–1166.
[18] E. Caurier, F. Nowacki, A. Poves, J. Retamosa, Phys. Rev. C 58 (1998) 2033–2040.
[19] A. Navin, D.W. Anthony, T. Aumann, T. Baumann, D. Bazin, et al., Phys. Rev. Lett. 85 (2000) 266–269.
[20] A. Ozawa, T. Kobayashi, T. Suzuki, K. Yoshida, I. Tanihata, Phys. Rev. Lett. 84 (2000) 5493–5495.
[21] C.R. Hoffman, T. Baumann, D. Bazin, J. Brown, G. Christian, et al., Phys. Rev. Lett. 100 (2008) 152502.
[22] R. Kanungo, C. Nociforo, A. Prochazka, T. Aumann, D. Boutin, et al., Phys. Rev. Lett. 102 (2009) 152501.
[23] J.I. Prisciandaro, P.F. Mantica, B.A. Brown, D.W. Anthony, M.W. Cooper, et al., Phys. Lett. B 510 (2001) 17–23.
[24] D.-C. Dinca, R.V.F. Janssens, A. Gade, D. Bazin, R. Broda, et al., Phys. Rev. C 71 (2005) 041302.
[25] A. Gade, R.V.F. Janssens, D. Bazin, R. Broda, B.A. Brown, et al., Phys. Rev. C 74 (2006) 021302.
[26] F. Wienholtz, D. Beck, K. Blaum, C. Borgmann, M. Breitenfeldt, et al., Nature 498 (2013) 346–349.
[27] M. Rosenbusch, P. Ascher, D. Atanasov, C. Barbieri, D. Beck, et al., Phys. Rev. Lett. 114 (2015) 202501.
[28] S.N. Liddick, P.F. Mantica, R.V.F. Janssens, R. Broda, B.A. Brown, et al., Phys. Rev. Lett. 92 (2004) 072502.
[29] D. Steppenbeck, S. Takeuchi, N. Aoi, P. Doornenbal, M. Matsushita, et al., Nature 502 (2013) 207–210.
[30] G. Hagen, M. Hjorth-Jensen, G.R. Jansen, R. Machleidt, T. Papenbrock, Phys. Rev. Lett. 109 (2012) 032502.
[31] H. Hergert, S.K. Bogner, T.D. Morris, S. Binder, A. Calci, et al., Phys. Rev. C 90 (2014) 041302.
[32] D. Steppenbeck, S. Takeuchi, N. Aoi, P. Doornenbal, M. Matsushita, et al., Phys. Rev. Lett. 114 (2015) 252501.
[33] M. Grasso, Phys. Rev. C 89 (2014) 034316.
[34] E. Yüksel, N. Van Giai, E. Khan, K. Bozkurt, Phys. Rev. C 89 (2014) 064322.
[35] J.J. Li, J. Margueron, W.H. Long, N. Van Giai, Phys. Lett. B 753 (2016) 97–102.
[36] S. Michimasa, M. Kobayashi, Y. Kiyokawa, S. Ota, D.S. Ahn, et al., Phys. Rev. Lett. 121 (2018) 022506.
[37] Y. Utsuno, T. Otsuka, Y. Tsunoda, N. Shimizu, M. Honma, et al., JPS Conf. Proc. 6 (2015) 010007.
[38] J. Erler, N. Birge, M. Kortelainen, W. Nazarewicz, E. Olsen, et al., Nature 486 (2012) 509.
[39] J.P. Delaroche, M. Girod, J. Libert, H. Goutte, S. Hilaire, et al., Phys. Rev. C 81 (2010) 014303.
[40] A.V. Afanasjev, S.E. Agbemava, D. Ray, P. Ring, Phys. Lett. B 726 (2013) 680–684.
[41] J.J. Li, W.H. Long, J.L. Song, Q. Zhao, Phys. Rev. C 93 (2016) 054312.
[42] G. Burgunder, O. Sorlin, F. Nowacki, S. Giron, F. Hammache, et al., Phys. Rev. Lett. 112 (2014) 042502.
[43] A. Mutschler, A. Lemasson, O. Sorlin, D. Bazin, C. Borcea, et al., Nat. Phys. 13 (2017) 152–156.
[44] O.B. Tarasov, T. Baumann, A.M. Amthor, D. Bazin, C.M. Folden III, et al., Phys. Rev. C 75 (2007) 064613.
[45] A. Gade, P. Adrich, D. Bazin, B.A. Brown, J.M. Cook, et al., Phys. Rev. Lett. 102 (2009) 182502.

[46] P. Baumann, A. Huck, G. Klotz, A. Knipper, G. Walter, Phys. Lett. B 228 (1989) 458–462.
[47] E. Caurier, F. Nowacki, A. Poves, Phys. Rev. C 90 (2014) 014302.
[48] B. Bastin, S. Grévy, D. Sohler, O. Sorlin, Z. Dombrádi, et al., Phys. Rev. Lett. 99 (2007) 022503.
[49] S. Takeuchi, M. Matsushita, N. Aoi, P. Doornenbal, K. Li, et al., Phys. Rev. Lett. 109 (2012) 182501.
[50] M. Grasso, L. Gaudefroy, E. Khan, T. Nikšić, J. Piekarewicz, et al., Phys. Rev. C 79 (2009) 034318.
[51] B. Schuetrumpf, W. Nazarewicz, P.-G. Reinhard, Phys. Rev. C 96 (2017) 024306.
[52] W.H. Long, P. Ring, N. Van Giai, J. Meng, Phys. Rev. C 81 (2010) 024308.
[53] S.-G. Zhou, J. Meng, P. Ring, Phys. Rev. C 68 (2003) 034323.
[54] J.F. Berger, M. Girod, D. Gogny, Nucl. Phys. A 428 (1984) 23–36.
[55] W.H. Long, H. Sagawa, N.V. Giai, J. Meng, Phys. Rev. C 76 (2007) 034314.
[56] L.J. Jiang, S. Yang, B.Y. Sun, W.H. Long, H.Q. Gu, Phys. Rev. C 91 (2015) 034326.
[57] E. Khan, M. Grasso, J. Margueron, N. Van Giai, Nucl. Phys. A 800 (2008) 37–46.
[58] M. Bender, K. Rutz, P.-G. Reinhard, J.A. Maruhn, W. Greiner, Phys. Rev. C 60 (1999) 034304.
[59] J. Dechargé, J.-F. Berger, K. Dietrich, M.S. Weiss, Phys. Lett. B 451 (1999) 275–282.
[60] P. Jerabek, B. Schuetrumpf, P. Schwerdtfeger, W. Nazarewicz, Phys. Rev. Lett. 120 (2018) 053001.
[61] H. Nakada, K. Sugiura, J. Margueron, Phys. Rev. C 87 (2013) 067305.
[62] J.M. Yao, S. Baroni, M. Bender, P.-H. Heenen, Phys. Rev. C 86 (2012) 014310.
[63] J.M. Yao, H. Mei, Z.P. Li, Phys. Lett. B 723 (2013) 459–463.
[64] See http://www.astro.ulb.ac.be.
[65] P.-G. Reinhard, H. Flocard, Nucl. Phys. A 584 (1995) 467–488.
[66] J. Meng, K. Sugawara-Tanabe, S. Yamaji, P. Ring, A. Arima, Phys. Rev. C 58 (1998) R628–R631.
[67] J. Meng, K. Sugawara-Tanabe, S. Yamaji, A. Arima, Phys. Rev. C 59 (1999) 154–163.
[68] W.-H. Long, N. Van Giai, J. Meng, Phys. Lett. B 640 (2006) 150–154.
[69] W. Long, H. Sagawa, J. Meng, N. Van Giai, Europhys. Lett. 82 (2008) 12001.
[70] G.A. Lalazissis, T. Nikšić, D. Vretenar, P. Ring, Phys. Rev. C 71 (2005) 024312.
[71] W. Long, J. Meng, N.V. Giai, S.-G. Zhou, Phys. Rev. C 69 (2004) 034319.
[72] J.J. Li, W.H. Long, J. Margueron, N. Van Giai, Phys. Lett. B 732 (2014) 169–173.
[73] J. Dobaczewski, W. Nazarewicz, T.R. Werner, J.F. Berger, C.R. Chinn, et al., Phys. Rev. C 53 (1996) 2809–2840.
[74] W. Pöschl, D. Vretenar, G.A. Lalazissis, P. Ring, Phys. Rev. Lett. 79 (1997) 3841–3844.
[75] A. Pastore, J. Margueron, P. Schuck, X. Viñas, Phys. Rev. C 88 (2013) 034314.
[76] M. Belabbas, J.J. Li, J. Margueron, Phys. Rev. C 96 (2017) 024304.
[77] J. Margueron, E. Khan, Phys. Rev. C 86 (2012) 065801.
[78] J.J. Li, J. Margueron, W.H. Long, N. Van Giai, Phys. Rev. C 92 (2015) 014302.
[79] Y.F. Niu, Z.M. Niu, N. Paar, D. Vretenar, G.H. Wang, et al., Phys. Rev. C 88 (2013) 034308.
[80] N.Q. Hung, N.D. Dang, Phys. Rev. C 78 (2008) 064315.
[81] D. Gambacurta, D. Lacroix, N. Sandulescu, Phys. Rev. C 88 (2013) 034324.
[82] Y.R. Shimizu, J.D. Garrett, R.A. Broglia, M. Gallardo, E. Vigezzi, Rev. Mod. Phys. 61 (1989) 131–168.
[83] D.J. Dean, M. Hjorth-Jensen, Rev. Mod. Phys. 75 (2003) 607–656.
[84] O.B. Tarasov, D.S. Ahn, D. Bazin, N. Fukuda, A. Gade, et al., Phys. Rev. Lett. 121 (2018) 022501.